IJRRS
International Journal of Reliability, Risk and Safety: Theory and Application

Online ISSN: 2676-3346

Vol. 6/ Issue 1/ 2023/ pp. 19-25
DOI: 10.22034/IJRRS.2023.6.1.3
Received: 31 May 2023, Revised: 19 July 2023 Accepted: 22 July 2023
Available online at: https://www.ijrrs.com

Case Study

In Situ Switch Blade Displacement Measurements in A Railway Turnout for Short-Term Monitoring Application

Kaveh Mehrzad [1*] and Shervan Ataei[2]

1. Arvand Barzin Knowledge Enterprise, Tehran, Iran

2. School of Railway Engineering, Iran University of Science and Technology, Tehran, Iran

*** kaveh906@yahoo.com**

Abstract

Due to the importance of the fundamental role of turnouts in network operations and their higher vulnerability than other assets, turnout condition monitoring is necessary for reliability-centered maintenance. Along with periodic visual inspections, real-time infrastructure condition detection can help introduce the structure's performance so that infrastructure maintenance is more reliable. A new approach for railway turnout pass-by condition detection is provided based on statistical process control (SPC) of damage-sensitive features (DSF) using switchblade lateral displacement (BLD) measurements. BLD time series data is modeled using a neural network model to extract DSF. This approach is applied to 33 passenger trains. The results of the proposed approach are validated by analysis of BLD and switch rod force sensor outputs. This method can be applied in turnout short-term condition monitoring for condition detection, leading to preventive maintenance, proper track operation management, and increased reliability.

Keywords: Blade displacement; Condition monitoring; Reliability centered maintenance; Railway turnout; Switch panel.

1. Introduction

Turnouts are vital elements of the rail network as they are responsible for guiding rail traffic. Due to the certain geometry of rail and complicated interaction of train-track in switch and crossing panels of turnout, these parts are very attractive in studies to prevent failure in railway systems. There are several studies to simulate the dynamics of the vehicle's passage over the crossing panel [1-3] and field measurements of the crossing panel [4-6] to investigate impacts induced in crossing by vehicle passing. A method to investigate the dynamic response of railway crossing based on acceleration and strain measurements was introduced in [4]. In another field study using nose rail acceleration measurements, impact acceleration was introduced as an indicator for evaluating crossing conditions [5]. Wheelset lateral displacements were measured in a study, and critical wheelsets were specified in switch and crossing panels by comparing measured displacements with frequency in switch and crossing panels [6].

Unlike the crossing panel in the switch panel area, relatively little numerical fieldwork has been done in the technical literature. However, this area is also a sensitive and accident-prone area due to the complex interaction of wheels and rails and is of great importance in terms of maintenance. Wear of switch/stock rail, soft spots, and plastic deformations are common failures/defects in switch panels [7].

Some numerical studies in switch panels were presented in [8-9]. In [8], a numerical study investigated the effect of the vertical relative motion of stock/switch rails onwheel–rail contact mechanics. Different non-Hertzian modeling approaches in wheel/rail contact problems were evaluated in [9]. From the numerical works, it can be found that the contact between the wheel and the rail is complex in the switch panel and is associated with the impacts caused by the wheel transfer from the stock rail to the blade rail.

In the static state, the gap between the blade and the stock rail in the close position is a key parameter of the switch health, and in some standards, such as [10], certain limits have been set for this parameter. However, this parameter has not been limited in the dynamic state while the train passes from turnout. The blade vibration caused by the contact forces of the wheels occurs due to the placement of the blade on the switch base plate. Therefore, measuring the size and pattern of blade displacements can measure the turnout interaction response to vehicle passage.

How to cite this article:
K. Mehrzad and Sh. Ataei. "In Situ Switch Blade Displacement Measurements in A Railway Turnout for Short-Term Monitoring Application," *International Journal of Reliability, Risk and Safety: Theory and Application*, vol. 6, no. 1, pp. 19-25, 2023.

This study uses Monitored BLDs to identify the condition of wheel/rail interactions in switch panels due to passing vehicles.

The use of statistical process control (SPC) methods in vibration-based fault detection is a common method in literature review. Reference [11] uses a statistical process control framework to support structural health monitoring in a historic building. In that study, an Autoregressive (AR) model fitted to the time history of acceleration measured in a sound structure is used. Residual values (forecast and measurement difference) are damage-sensitive (DSF) features. In [12], the AR Support Vector Machines (SVM) method is used instead of the AR linear model. In terms of control ability in nonlinear dynamics and the structure of the model, a nonlinear time series model is proposed. [13] It also proposes a technique based on the residual moving average regression model of exogenous inputs (ARMAX) to improve noise and damage detection power in different types of stimuli and realistic conditions in the shear structure. In most of the mentioned studies, the damage identification is supervised type due to the possibility of applying damage with different degrees. Because in most cases, like the turnout survey in this study, the data available is only from a sound structure, damage detection must perform in an unsupervised form. In this study, condition detection in an unsupervised method is conducted using the control chart method on residuals of Non-linear AR neural network (NN) prediction models.

First, the data source used in this study is described. Then the method for modeling of time series is presented. The results of condition detection during train passages are presented in the fourth section, and validation of the detected trains has been done by statistical analysis of the data of different sensors. Figure 1 shows a diagram of the methodology of this study.

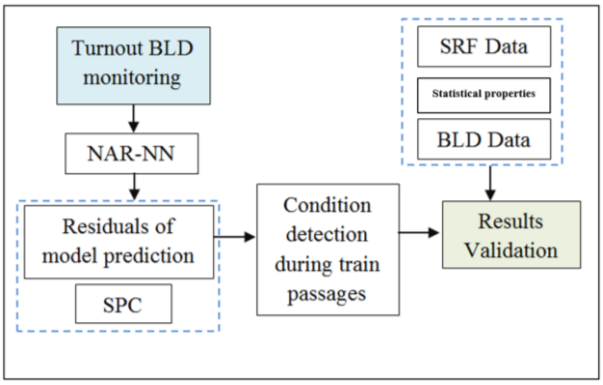

Figure 1. Diagram of research methodology

2. Data source

2.1 Field measurement

Generally, a turnout is formed from a switch panel, a closure panel, and a crossing panel (figure 2(a)). In a case study, the entrance turnout in the mainline of one station was instrumented, and the turnout was monitored [14, 15]. The turnout is a 1:9 left-hand turn out with a 60E1 full rail section type.

Figure 2(a) illustrates the location of train detection sensors, including the axle counter (Trigger) sensor, Weigh In Motion (WIM) sensor to detect train properties, and switchblade lateral displacement (BLD) sensor in the turnout plan view. Figure 2(b) shows the hardware part of the turnout monitoring system. Data were measured in the mainline and the facing direction of the turnout. The measurement sampling frequencies of the sensors are 10 kHz. Measurements include signals from consecutive passage of 33 trainsets passenger trains in two months.

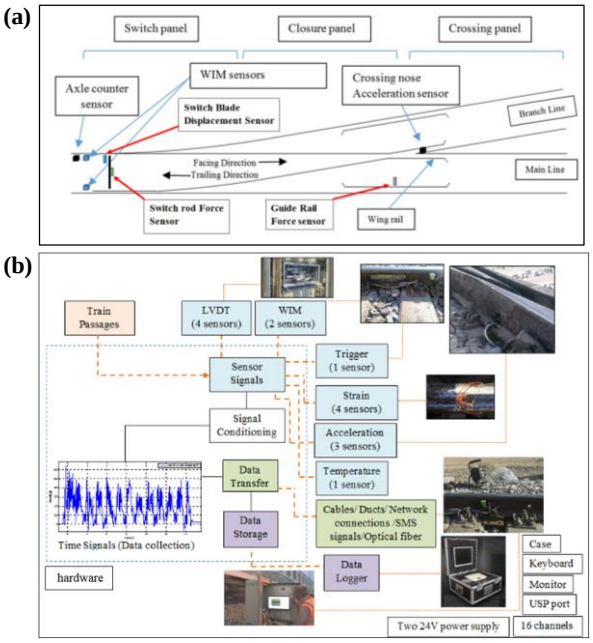

Figure 2. Instrumentation of turnout, **(a)** General layout of turnout and sensors configuration, **(b)** The hardware of the turnout monitoring system

2.2 Data Processing

In the first step, passing train characteristics are determined by processing the axle counter sensor and WIM sensor data. Dynamic axle load and train configuration from raw data could be detected according to Figure 3(a).

Trainsets have more uniform specifications [16], including axial load and speed, number, and axle distance, and therefore, they have more comparative conditions to check for fault detection. Therefore, these train passages were selected from numerous vehicle data.

To reduce the volume of data to introduce to the forecasting AR model, signal preprocessing, reducing sample frequency from 10 kHz to 100 Hz, was performed in BLD data.

The measured data from WIM sensors for a train-set passage (train No. 20) with 5 self-traction units (20 axle passage) at 116 km/h speed are shown in Figure 3(b). To uniformize all data series, the middle part of the trains, including the passage of four P.Bogies, has been included in the continuation of the study (figure 3 b).

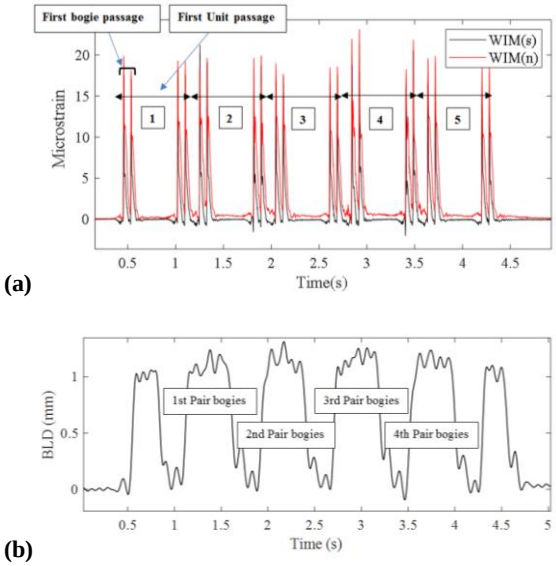

Figure 3. Train specification detection, **(a)** Train configuration detection by WIM sensor outputs, **(b)** First to 4th P.Bogies effects on BLD measurement data

Based on the time of train passage from turnout, trains were classified, and six groups of trains were detected (G1 to G6). Thirty−three train sets were selected for applying the methodology.

The statistical specifications of the studied trains containing estimated train axle load, speed, and BLD are presented in Figure 4 (a, b, and c), respectively.

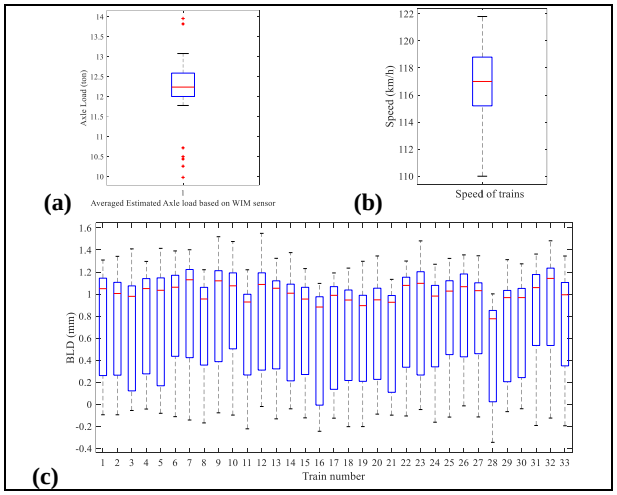

Figure 4. The statistical specifications of the studied trains containing **(a)** Train axle load, **(b)** Speed, and **(c)** BLD

2.3 Time series prediction method

Predictive models are used to identify systems when dynamic models are created from physical systems. These dynamic models are important for analyzing, simulating, monitoring, and controlling various systems [17]. In this study, the time series forecasting model is applied to identify train passings with potential failures.

2.4 Nonlinear Auto Regressive Neural network (NAR-NN)

Dynamic Neural Networks (DNN), which include delay lines, are used for nonlinear filtering and prediction. These networks perform well in predicting time history. The view of the desired network is shown in Figure 5.

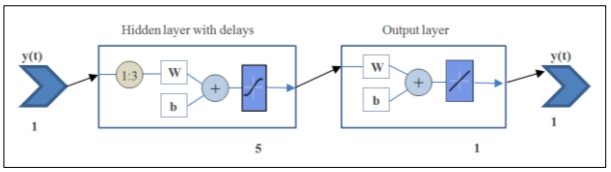

Figure 5. Structure of a nonlinear autoregressive neural network

Future values of time history y (t) are estimated from the previous values of the series. This form of nonlinear autoregressive prediction, or NAR, can be written as follows:

$$y(t) = f(y(t-1), \ldots, y(t-d)) \quad (1)$$

Based on equation 1, in NAR prediction, the future values y (t) of a time series are predicted only from d past values/or delays of that series.

The trial and error method has been used to create the optimal neural network structure. According to many similar studies, a hidden layer for NN with a sufficient number of neurons provides a comprehensive estimator. Levenberg–Marquardt, a powerful learning algorithm, was used here.

The Log-Sigmoid Transfer Function and Linear Transfer Function were selected for the hidden and output layers. The optimal network structure was selected by minimizing the error. The learning pause is set until the error reaches an acceptable level or the predetermined number of epochs.

Potential inputs for autoregressive neural network models from one to three previous data (Y(t-1), Y(t-2), Y(t-3)) checked out. The selection of the optimal structure is based on the training process on the first 50% and the test error on the second 50% of one of the passing train BLD data (train No. 50). A commonly used train and test data ratio is 80:20. Other ratios such as 70:30, 60:40, and even 50:50 are also used in practice [18]. In this study, according to the number of over 400 data in a data series, 50% of the data were found to be sufficient for training. Similarly, by changing the characteristics of the neural network model (number of neurons and changing inputs), the model performance results were extracted, which are presented in Figure (6). Performances of models were evaluated by mean square error. According to Figure (6), the neural network with 5 neurons and 3 previous inputs (three delays) is the superior option.

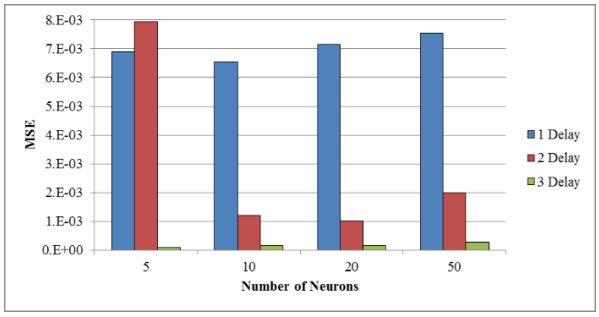

Figure 6. Effect of the number of neurons and delays on the performance of the NAR-NN model

3. Results and discussion

3.1 Control chart results

Based on Shewhart's theory, all processes, although in a healthy state, are detected with a certain amount of change if measured with a sufficiently accurate instrument. When this variability is limited to random changes, the process is called static control. Also, if the variability of the process is affected by a specific factor such as incorrect machine settings, incorrect operation, insufficient raw materials, worn machine components, etc., in this case, the process will be out of static control. These determinants of change usually have a detrimental effect on product quality, so it is important to have systematic techniques for identifying these important deviations from statistical control as soon as they occur. Control charts are primarily used for this purpose. Control Charts can distinguish certain (determinable) factors from random changes. Therefore, this method can be used to troubleshoot to identify the cause of out-of-control conditions [19, 20].

In this study, a control chart has been used for individual measurements. Each sample is considered an observation, and the moving range (MR) of two consecutive samples (sample size, n=2) is used to estimate process variability. MR, Up Control Limit (UCL), and Low control limit (LCL) is estimated from equation 2 using residuals (x) values of prediction models.

$$MR\_i = |x\_i - x\_(i-1)|$$
$$UCL = D_4\overline{MR} \quad (2)$$
$$LCL = D_3\overline{MR}$$

$\overline{MR}$ is the average of MR, and the values of D_3 and D_4 per sample size are available in reference books. More detailed information about the statistical theory of equations can be found in the reference [20]. Given that, in this case, each data is correlated with the previous data, the presence of a trend in the MR chart does not necessarily indicate an error.

Before calculating the control limits, it must first be determined from which train these limits will be calculated. The representative train should generate the lowest vibration levels to make it easier to identify irregularly passing trains. For this purpose, the maximum values of blade vibration caused by trains have been re-evaluated. Train number 464, with the lowest maximum BLD, was selected as the base train to calculate the statistical control limits. Figure (7-a) shows the blade vibration caused by the passage of this train. The prediction results of the NN model and the residual values for train No. 464 are shown in Figure (7-b).

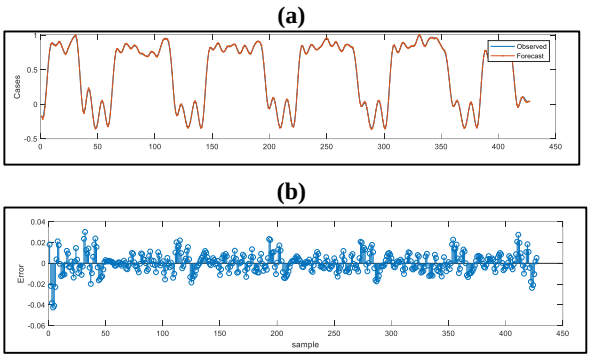

Figure 7. (a) Forecast and **(b)** Residual Values - Train No. 464

Here is an example of the results for the range of residual values of trains group 6 in Figure 8. As shown in Figure 8, trains 680 and 646 have values beyond the statistical control limit in the second and first P. Bogie, respectively.

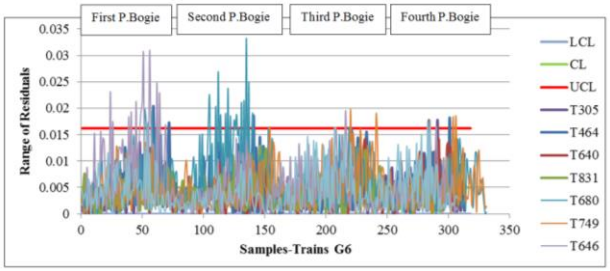

Figure 8. Results of R-chart analysis of trains group 6

Box plot analysis was performed on the OOC points to identify critical trains, and the results are shown separately by the location of the bogie pairs in Figure 9. The allowable number of OOCs is considered equal to the outlier limit in the total case of OOCs. According to the results, trains 646, 680, and 268 are the worst cases in the first, second, and fourth P. Bogie, respectively. The highest number of OOCs was identified on train number 680. The cases of trains detected in the previous are summarized in Table (1).

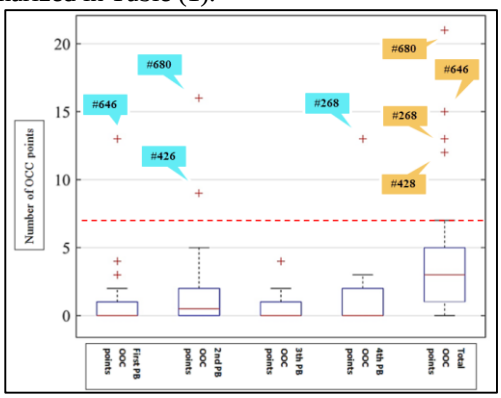

Figure 9. Box plot analysis of OOC cases for identification of worst train passages

Table 1. Trains detected by the proposed method

1st P. Bogies	2nd P. Bogies	4th P. Bogies	Total
646	680	268	680
-	426	-	646
-	-	-	268

The detected trains as potentially defective train passages are validated by examining the values of the BLD sensor and other instrumented sensors in the turnout.

3.2 Validation of train condition detection results

The results have been validated by reviewing and comparing the outputs of two sensors, including BLD and switch rod force (SRF).

a) BLD sensor

For comparison, the displacement of the blade of train No. 50 as a normal passage is compared with the data obtained from the passage of train No. 680. As can be seen, the sensor recorded small values of about 0.1 to 0.2 mm in the middle areas between the passages of the P.Bogies (figure 10a). However, the displacement of the blade due to the passage of train No. 680 shows the values of intense vibration after the passage of the first and fourth P.Bogies, which can reach up to 1 mm (figure 10b).

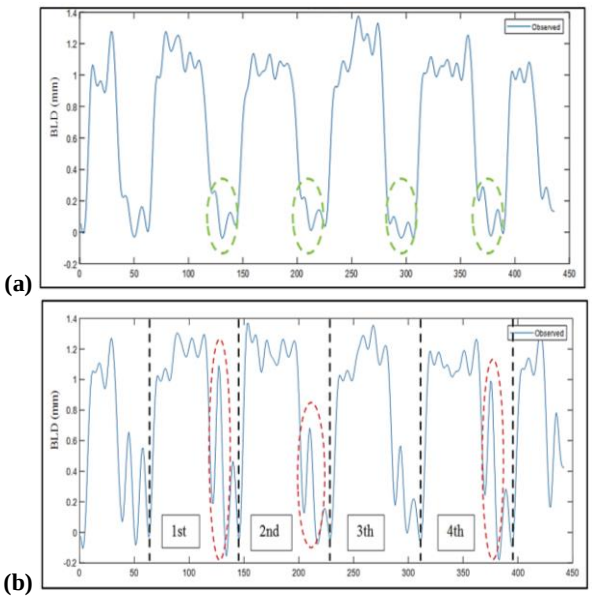

Figure 10. Comparison of BLD measurement **(a)** Blade vibration due to the passage of train No. 50 as a normal passage **(b)** Blade vibration caused by passing train No. 680

To compare all the trains, after synchronizing the blade displacement signals, values were plotted for all eight vibration zones caused by the train passing in Figure 11, and maximum values were identified. These eight areas include the passage of 4 P.Bogies (1, 3, 5, 7 areas in Figure 11) and 4 middle zones (M-zones containing 2, 4, 6, 8 in Figure 11) for a train-set with 5 self-traction wagons.

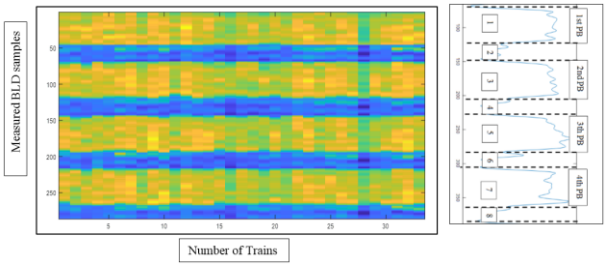

Figure 11. Blade vibration due to the passage of all trains

The eight areas mentioned are evaluated, and trains that match the trains detected by the statistical control method are shown in Figure 12 (a, b, and c) for the first, second, and fourth M-zones, respectively. Finally, train No. 680, 646, 426, and 628 were detected by this method.

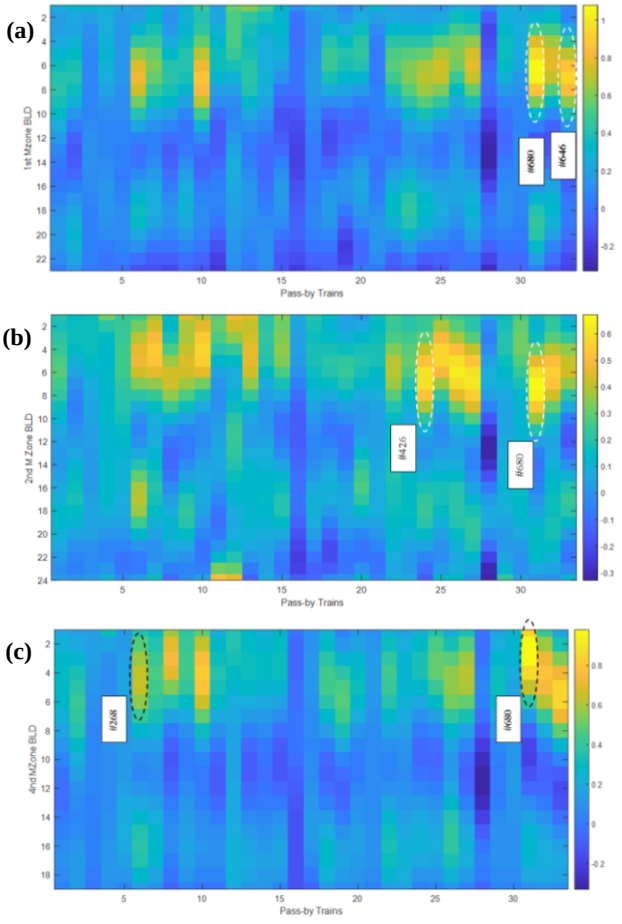

Figure 12. Blade vibration during the passage of all trains **(a)** First M-zone **(b)** Second M-zone **(c)** Fourth M-zone

b) Switch rod force sensor

Another signal that was examined to validate the detection results of irregularly passing trains is the switch rod force. To show the effect of passing each wheel on the position of the switch rod, trigger signals, and the switch rod force signals were aligned. In figure (13), the effect of each wheel's impact on the switch rod's force and fluctuations after passing the pair of bogies is well known. Figure (14) shows the effect of passing the bogies of all trains on the switch rod force.

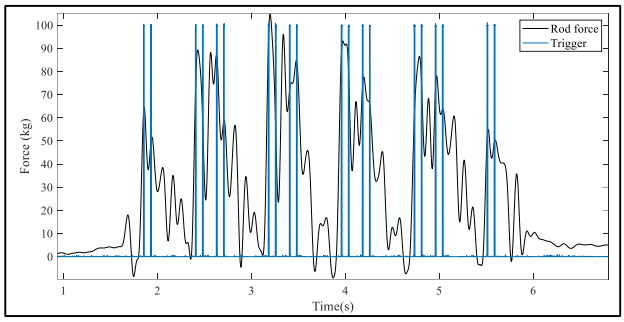

Figure 13. Aligned signals of trigger and force of the switch rod

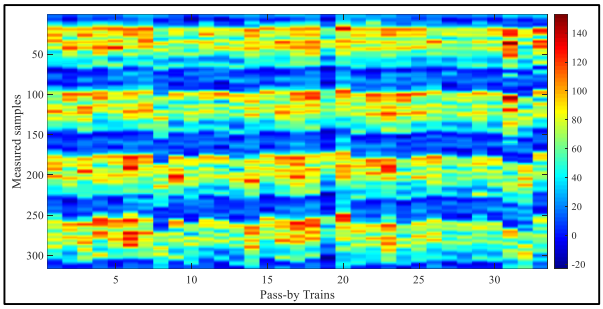

Figure 14. Effect of passing the bogies of all trains on the force of the switch rod

Here, three statistical parameters have been used for more efficient comparison between trains, including standard deviation, mean and minimum to maximum. Figure 15 (a, b, and c) shows the statistical parameters for the passage of the trains' first, second and fourth P.Bogies, respectively.

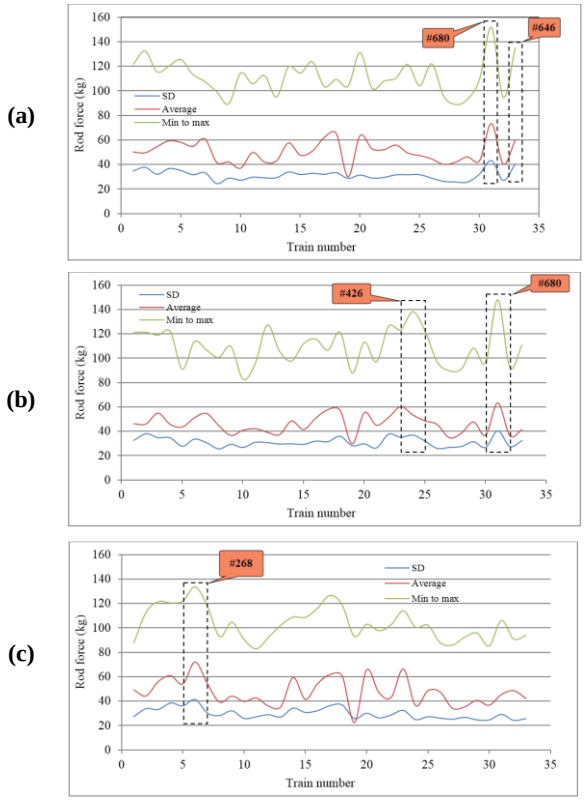

Figure 15. SRF Statistical parameters for the passage of **(a)** First P.Bogie **(b)** Second P.Bogie **(c)** Fourth P.Bogie

In summary, five trains detected by statistical sensors output investigation of the SRF. Table 2 shows results that confirm the control chart method by the statistical analysis of the sensors. The location of irregularities/defects is also included in the investigation. Therefore, trains, including 680, 646, 426, and 268, were detected by statistical evaluation of sensor values, which confirms the control charts method using the NN method.

Table 2. Trains detected by two methods of control chart and sensors output investigation

Sensors output investigati	Control chart method	Sensor Output	Location on the train		
			1st P.Bogies	2nd P.Bogies	4th P.Bogies
NA	NAR-NN	BLD	646-680	426-680	268
Max	NA	BLD	646-680	426-680	680-268
Min to Max	NA	SRF	680	680	268

Due to the results in all cases, the trains identified by the statistical control method are compatible with statistically examining the output of the sensors.

4. Conclusion

This study used switchblade lateral displacement data to monitor the vibration and wheel shocks caused by irregular and potentially defective train passing. Using the neural network method, the time history of blade displacements has been modeled. BLD time series data is modeled using a neural network model to extract DSF. Statistical method (Control Charts) has been used to identify the number and location of OOC cases. According to the results of this study, trains with destructive passage through the switch panel were identified. For the purpose of validation, the results were compared with two parallel methods, including statistical analysis of blade displacements and the switch rod force. In all cases, reviewing the results of the sensors confirmed the results obtained using the NN method. However, statistical maximum values alone cannot identify the desired trains. The main difference in blade vibration caused by the detected trains was the free vibration in the middle zone of the pair bogies crossing, which does not necessarily occur in trains with maximum blade vibration.

Along with periodic visual inspections, real-time infrastructure condition detection can help introduce the structure's performance so that maintenance is more reliable. The importance of this study is in presenting a new solution for identifying irregularly passing trains in the unsupervised method in railway switches. Applying this method, based on switch structure monitoring data, can improve and optimize the operation of different rolling stocks and thus reduce vehicle and line maintenance costs. The results can also be used in preventive maintenance to prevent the spread of breakdowns and injuries.

5. References

[1] M. Pletz, W. Daves, and H. Ossberger, "A wheel passing a crossing nose: Dynamic analysis under high axle loads using finite element modelling*," *Proceedings of the Institution of Mechanical Engineers, Part F: Journal of Rail and Rapid Transit*, vol. 226, no. 6, pp. 603-611, 2012, doi: https://doi.org/10.1177/0954409712448038.

[2] Y. Ma, A. A. Mashal, and V. L. Markine, "Modelling and experimental validation of dynamic impact in 1:9 railway crossing panel," *Tribology International*, vol. 118, pp. 208-226, 2018/02/01/ 2018, doi: https://doi.org/10.1016/j.triboint.2017.09.036.

[3] P. T. Torstensson, G. Squicciarini, M. Krüger, B. A. Pålsson, J. C. O. Nielsen, and D. J. Thompson, "Wheel–rail impact loads and noise generated at railway crossings – Influence of vehicle speed and crossing dip angle," *Journal of Sound and Vibration*, vol. 456, pp. 119-136, 2019/09/15/ 2019, doi: https://doi.org/10.1016/j.jsv.2019.04.034.

[4] M. A. Boogaard, Z. Li, and R. P. B. J. Dollevoet, "In situ measurements of the crossing vibrations of a railway turnout," *Measurement*, vol. 125, pp. 313-324, 2018/09/01/ 2018, doi: https://doi.org/10.1016/j.measurement.2018.04.094.

[5] X. Liu, V. L. Markine, H. Wang, and I. Y. Shevtsov, "Experimental tools for railway crossing condition monitoring (crossing condition monitoring tools)," *Measurement*, vol. 129, pp. 424-435, 2018/12/01/ 2018, doi: https://doi.org/10.1016/j.measurement.2018.07.062.

[6] G. Jing, M. Siahkouhi, K. Qian, and S. Wang, "Development of a field condition monitoring system in high speed railway turnout," *Measurement*, vol. 169, p. 108358, 2021/02/01/ 2021, doi: https://doi.org/10.1016/j.measurement.2020.108358.

[7] I. Grossoni, P. Hughes, Y. Bezin, A. Bevan, and J. Jaiswal, "Observed failures at railway turnouts: Failure analysis, possible causes and links to current and future research," *Engineering Failure Analysis*, vol. 119, p. 104987, 2021/01/01/ 2021, doi: https://doi.org/10.1016/j.engfailanal.2020.104987.

[8] X. Ma, P. Wang, J. Xu, and R. Chen, "Effect of the vertical relative motion of stock/switch rails on wheel–rail contact mechanics in switch panel of railway turnout," *Advances in Mechanical Engineering*, vol. 10, no. 7, p. 1687814018790659, 2018, doi: https://doi.org/10.1177/1687814018790659.

[9] X. Ma, P. Wang, J. Xu, and R. Chen, "Comparison of non-Hertzian modeling approaches for wheel–rail rolling contact mechanics in the switch panel of a railway turnout," *Proceedings of the Institution of Mechanical Engineers, Part F: Journal of Rail and Rapid Transit*, vol. 233, no. 4, pp. 466-476, 2019, doi: 10.1177/0954409718799825.

[10] *UFC 4-860-03 Railroad Track Maintenance And Safety Standard*, U. S. A. C. o. Engineer, 13 February 2008. [Online]. Available: https://www.wbdg.org/FFC/DOD/UFC/ufc_4_860_03_2008.pdf

[11] D. E. Kosnik, W. Zhang, and P. L. Durango-Cohen, "Application of Statistical Process Control for Structural Health Monitoring of a Historic Building," *Journal of Infrastructure Systems*, vol. 20, no. 1, p. 05013002, 2014, doi: https://doi.org/10.1061/(ASCE)IS.1943-555X.0000164.

[12] L. Bornn, C. R. Farrar, G. Park, and K. Farinholt, "Structural Health Monitoring With Autoregressive Support Vector Machines," *Journal of Vibration and Acoustics*, vol. 131, no. 2, 2009, doi: 10.1115/1.3025827.

[13] L. Mei, A. Mita, and J. Zhou, "An improved substructural damage detection approach of shear structure based on ARMAX model residual," *Structural Control and Health Monitoring*, vol. 23, no. 2, pp. 218-236, 2016, doi: https://doi.org/10.1002/stc.1766.

[14] K. Mehrzad, "Presenting a prediction model for the safe passage speed of the train through the main line of the turnout based on the measurement of mechanical and geometrical parameters using soft computing," Ph.D. dissertation, IUST university, 2022.

[15] K. Mehrzad and S. Ataei, "Railway crossing vertical vibration response prediction using a data-driven neuro-fuzzy model – Influence of train factors," *Proceedings of the Institution of Mechanical Engineers, Part F: Journal of Rail and Rapid Transit*, vol. 235, no. 9, pp. 1086-1098, 2021, doi: https://doi.org/10.1177/0954409720986666

[16] S. Ataei and K. Mehrzad, "Permanent condition Monitoring of Yatri P2 Station Report," *Intelligent monitoring of infrastructures Lab., Iran University of Science & Technology*, 2017.

[17] T. Hudson, B. Hagan, Deep Learning Toolbox, Getting Started Guide Mark, Version 14.4, MathWorks, Inc. 2022.

[18] V. R. Joseph, "Optimal ratio for data splitting," *Statistical Analysis and Data Mining: The ASA Data Science Journal*, vol. 15, no. 4, pp. 531-538, 2022, doi: https://doi.org/10.1002/sam.11583.

[19] W. C. Navidi, *Statistics for engineers and scientists*, 3th ed. New York: McGraw-Hill 2010.

[20] W. W. Hines, D. C. Montgomery, D. M. Goldsman, and C. M. Borror, *Probability and Statistics in Engineering*. Wiley, 2003.